Theoretical stability of the polarization in insulating ferroelectric/semiconductor structures

Watanabe, Yukio
Kyushu Institute of Technology

出版情報：Journal of applied physics. 83 (4), pp.2179-2193, 1998-02-15. American Institute of Physics
バージョン：

Theoretical stability of the polarization in insulating ferroelectric/semiconductor structures

Yukio Watanabe[a)]
Kyushu Institute of Technology, Kitakyushu, Fukuoka 804, Japan

(Received 6 October 1997; accepted for publication 3 November 1997)

Stability of the polarization in a thin ferroelectric film on a semiconductor is theoretically investigated using an insulating homogeneous Ginzburg–Landau theory. Dependence of the stability on various parameters such as the ferroelectric thickness, the materials ($BaTiO_3$, $KNbO_3$, $PbTiO_3$, $Bi_4Ti_3O_{12}$), the interfacial defects, the work function difference, the epitaxial orientation, and the buffer insulator thickness is numerically and analytically studied, and the results are qualitatively compared with the past experiments on ferroelectric field effect devices. The spontaneous polarization in a ferroelectric single-domain on a semiconductor is shown to be bistable in agreement with recent experiments. Furthermore, its thickness limit of the ferroelectric stability is found to be very small, implying a great potential of this structure for the miniaturization. The single-domained spontaneous polarization is destabilized when even a very thin insulating layer exists between the ferroelectric and the semiconductor. The formation of the multidomain is found to be insufficient to stabilize the spontaneous polarization in thin ferroelectrics used in experiments. The spontaneous polarization can be stabilized at one polarity by the defects or the surface states at the ferroelectric/insulator interface, which explains its temporary stability experimentally suggested. The thermodynamic liner susceptibility is crucial for the stability, while the ferroelectric stability is predicted to be enhanced by modifying it effectively by changing the epitaxial orientation of the ferroelectric film. An addition of metallic layer between the ferroelectric and the insulator changes this restriction, although this invites another instability of the conductance modulation. To explain the experimental instabilities, they are classified into four categories. The present study suggests also a limitation of the assumption of an insulating ferroelectric under a very large depolarization field. © *1998 American Institute of Physics.* [S0021-8979(98)01604-1]

I. INTRODUCTION

Advances in material preparations and methods to characterize small-scale-properties have clarified that finite size effect occurs much below the previous expectations. The size effect of displacive-type ferroelectric, e.g., $BaTiO_3$, has been an interest of a basic research.[1–16] Moreover, the effect in thin film is currently of a practical concern. For example, thermodynamic fluctuations pointed by Bell[2] can suppress the ferroelectricity in a small particle of about 1 nm in diameter.[3] This result encourages also the use of constants in Ginzburg–Landau-Devonshire (GL) theory for ferroelectric larger than this size. The surface effect described by an inhomogeneous GL theory[4–7] was suggested to produce the size effect even if the surface charge is compensated at the metallic electrodes.[8] Importance of multidomain formation was demonstrated in small particles *without electrodes*.[9–11] Enormous contribution of the incomplete surface charge compensation to the size effect was suggested by Batra *et al.*[12–16]

The ferroelectricity can be characterized by both lattice parameters and electrical properties. The most measurements of the electrical properties use *electrodes* or *contacts* between different particles that can kill the depolarization effect. This fact has been often overlooked, and the size effect of crystallographic properties, and the electrical properties such as the dielectric constant have sometimes been analyzed in the same way. Therefore, it is necessary to discuss the size effect of electrical properties of ferroelectric having a specific electrode material.

In commonly used measurements, it is difficult to sense directly the polarization without reversing it. Semiconductor electrodes can allow to measure directly its surface charge via conductance modulation and, thus, provide a unique opportunity to study the ferroelectric size effect and the surface polarization. Moreover, the carrier concentration and the conduction type can be arbitrarily selected. Additionally, this system has a practical importance as ferroelectric field effect transistors (ferroelectric FETs) or resistors.[17–32] In fact, this system has long been studied, and its limitation was warned by Batra *et al.*[14–16] By far, no approach has succeeded to realize it with conventional semiconductor materials. Therefore, the clarification of the physical feasibility of ferroelectric FETs and their miniaturization limit is desired.

Surface layers having crystallographic properties different from those of a bulk ferroelectric were often interpreted as a finite size effect by an inhomogeneous GL theory.[4] Disappearance of the ferroelectricity as detected by crystallographic symmetry and reduction of the dielectric constant were reported in a few hundred-nm-thick $BaTiO_3$ or $SrTiO_3$.[33,34] However, the results have been dependent on preparation methods and found .to be mostly due to an ex-

a)Electronic mail: ynabe@tobata.isc.kyutech.ac.ip

traneous effect.[35] In a novel approach, i.e., a use of single-crystallike epitaxial heterostructures that reduce interfacial defects and disorders, a 20-nm-thick $SrTiO_3$ film showed dielectric constant of 160 that is only a 15% decrease from the value at 150 nm.[36] Furthermore, a 14-nm-thick $BaTiO_3$ film exhibited crystallographic symmetry corresponding to a ferroelectric phase.[37] These experimental facts do not favor an inhomogeneous GL theory for size effect in ferroelectric films.

In this article, we report the stability of spontaneous polarization (P_s) in ferroelectric/x/semiconductor structures. For ferroelectric FETs, there are theories that deal with the conductance modulation characteristics.[38] However, few theoretical works on the stability have been known after the works by Batra *et al.*

We employ the following basic assumptions: (1) Single crystalline ferroelectric thin film layer. The top surface of the ferroelectric should have the same crystallographic quality, or atomic-bond energies. (2) Homogeneous GL theory for ferroelectric, disregarding the surface effect. (3) Insulating ferroelectric, no carrier generation in ferroelectric. In a separate article, the ferroelectric is treated as a semiconductor having a wide gap. (4) Boltzmann distribution and nonquantum mechanical treatment of charge carriers in the accumulation and the inversion region of a semiconductor.

In most part of this article, unidomain (single-domain) ferroelectric is assumed. Here, a *''unidomain'' means that the width of the domains of, at least, one polarity is much larger than the ferroelectric thickness and the space charge layer thickness.*

Using these assumptions, we examine the dependence of the instability on (i) the thickness of the ferroelectric and the insulating layer between the ferroelectric and the semiconductor, (ii) the ferroelectric material ($BaTiO_3$, $KNbO_3$, $PbTiO_3$, $Bi_4Ti_3O_{12}$) and the semiconductor materials (Si, Ge, GaAs), (iii) the temperature, the semiconductor-metal work function difference, the semiconductor doping concentration, the buffer insulator thickness, and the trap density at the ferroelectric/insulator interface.

The quantitative results in this article changes, when the semiconductor property of ferroelectric is considered (article II Ref. 39). However, the semiconductivity of the ferroelectrics in the size effect is not yet established and render the theory opaque. Therefore, we construct a basic frame work of our approach and use only established concepts and material parameters.

The following results and the results in article II can be translated to explain the size effect of the ferroelectric powder by neglecting the lateral size effect, when the surface layer of the powder is regarded as an insulator. Namely, a ferroelectric powder or a ferroelectric platelet can be modeled as $S/I/F/I/S$. In this case, the thickness of the ferroelectric film below (l_f) corresponds to the radius or half of the thickness of the ferroelectric core region of the powder.

The subsequent part of the article is organized as (2) formulation of the stability, (3) approximate analytical results and guiding principles, (4) numerical results, (5) multidomain effect, and (6) effect of defects and disorder, and comparison with experiments.

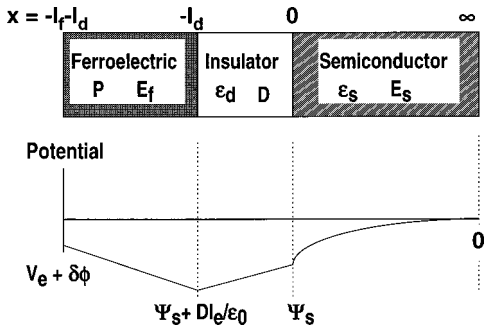

FIG. 1. $F/I/S$ structure and distribution of potential.

II. FORMULATION OF THE PROBLEMS AND ASSUMPTIONS

A. Formulation

We consider the structure as in Fig. 1, where l_f and l_d are the thickness of the ferroelectric and the insulating layer, respectively. The x coordinate is defined in the direction perpendicular to the film, where $x=0$ is at the boundary between the insulator and the semiconductor. For a while, we do not include the effect of the disorder and defects at the interface, of which effect is discussed in Sec. V.

This model corresponds to an artificially formed multilayer and also to other structures. In one of them, a ferroelectric/semiconductor (F/S) structure can also represent the ferroelectric having a dead layer that lost the ferroelectricity. Similarly, ferroelectric/insulator/semiconductor ($F/I/S$) structure can also correspond to the ferroelectric/semiconductor structure having a dead layer on the ferroelectric surface.

For a $F/I/S$, the polarization (P) dependent part of free energy density $F(\text{per cm}^3)$ is written as

$$F=F_f(P)+F_d(P)/l_f+F_s(P)/l_f, \tag{1}$$

where F_f, F_d, and F_s, corresponds to the free energies of the ferroelectric, the insulator, and the semiconductor, respectively.

The F_f for $BaTiO_3$, and $KNbO_3$, and $PbTiO_3$ is written as:

$$F_f=\alpha_1 P^2+\alpha_{11}P^4+\alpha_{111}P^6+\eta(\nabla P)^2-\int_0^P dPE_f, \tag{2''}$$

where $E_f \equiv E_f(P)$ is the electric field in the ferroelectric, and a unidomain is assumed.[40–42] The inverse of the linear susceptibility α_1 is written as $\alpha_1=(T-\theta)/2\epsilon_0 C$, where θ and T are the Curie temperature (T_c) and the ambient temperature, respectively. The c-axis of the ferroelectrics, i.e., the direction of P, is assumed to be perpendicular to the film surface. The last integral in Eq. (2″) is the depolarization term which follows the conventional expression. For $\nabla P \neq 0$, Eq.(2″) needs to be integrated from $x=-l_f-l_d$ to $x=-l_d$ and then divided by l_f.

To treat all the energies consistently, we express the depolarization term by an electrostatic field energy. We consider an infinitesimal change of dipole moment of $p, \delta p$, in one-dimensional $F/I/S$, where p and δp are directed to the interface with angle of φ ($0° \leqslant \varphi < 90°$; ex. $\varphi=0° \Leftrightarrow c$-axis-oriented film), and p corresponds to P in ferroelectric. A detailed derivation is reported in Appendix C

TABLE I. GL parameters in Eqs. (2) and (2b) adopted from Refs. 41–43.

	θ (°C)	C (°C)	α_{11} (JC^{-4} cm^8)	α_{111} (JC^{-6} cm^{12})
$PbTiO_3$	478.8	1.5×10^5	-7.252×10^{17}	2.606×10^{26}
$KNbO_3$	418	2.4×10^5	-4.05×10^{18}	2.989×10^{27}
$BaTiO_3$	96.9	1.7×10^5	-1.377×10^{18}	2.77×10^{27}
$Bi_4Ti_3O_{12}$	(all in esu, T in °C)			

α_1	α_3	α_{11}	α_{33}	α_{12}
$2.85\times10^{-5}\ (T-540)$	0.04334	-1.06×10^{-12}	1.3×10^{-10}	$-2.17\times10^{-15}T+1.4\times10^{-12}$
α_{13}	α_{111}	α_{333}	α_{3333}	
$-3.22\times10^{-15}\ T-4.258\times10^{-12}$	9.56×10^{-23}	-1.2×10^{-19}	4.52×10^{-28}	

of article II.[39] Charges are only in the semiconductor and the ferroelectric. Using the notations in Fig. 1, the change of the electrostatic energy is

$$\int_0^\infty dx\,\delta\rho(x,p)\Psi(x,p)-E_f\delta p\,\cos\varphi l_f$$

$$=[\epsilon_s\epsilon_0\delta E(x,p)\Psi(x,p)]_0^\infty+\epsilon_s\epsilon_0\int_0^\infty dx\,\delta E(x,p)E(x,p)$$

$$-E_f\delta p\,\cos\varphi l_f,$$

where $\Psi(x,p)$, E_f, δE, and δp are the electrostatic potential at x for $p=p$, the electric field in the ferroelectric, the changes of E and ρ due to δp, respectively.

The potential at $x=0$ and $x=\infty$ are

$$\Psi(0,p)=-Dl_d/\epsilon_d\epsilon_0-E_fl_f+\Psi(x=-l_f-l_d),$$

$$\Psi(\infty,p)=0.$$

Using these relations, $\epsilon_s\epsilon_0\delta E(0,p)=\delta D$ and $\delta D=\delta p\,\cos\varphi+\epsilon_0\delta E_f$, we have

$$=-\delta D[-Dl_d/\epsilon_d\epsilon_0-E_fl_f+\Psi(x=-l_f-l_d)]$$

$$+\epsilon_s\epsilon_0\int_0^\infty dx\,\delta E(x,p)E(x,p)-E_f(\delta D-\epsilon_0\delta E_f)l_f$$

$$=\delta\Bigg[D^2(p)l_d/2\epsilon_d\epsilon_0+\epsilon_s\epsilon_0/2\int_0^\infty dxE^2(x,p)$$

$$+\epsilon_0E_f^2(p)l_f/2-D(p)\Psi(x=-l_f-l_d)\Bigg],$$

where $\delta[\ ]$ means the change of the value inside of [ ] due to δp. The last expression is the change of the field energy stored in $F/I/S$ due to δp. The final relation is obtained by integrating the first and the last expressions from $p=0$ to $p=P$. We disregard $p=0$ terms because we are interested in the P-dependent part of F and but not in an absolute value of F.

Using the above results, we express F_f, F_d, and F_s by an electrostatic field energy.

$$F_f=\alpha_1P^2+\alpha_{11}P^4+\alpha_{111}P^6+\eta(\nabla P)^2+\epsilon_0E_f^2/2$$

$$-D\Psi(x=-l_f-l_d)l_f$$

$$=F_0+\eta(\nabla P)^2+\epsilon_0E_f^2/2-D\Psi(x=-l_f-l_d)/l_f, \qquad (2)$$

$$F_d=l_eD^2/2\epsilon_0, \qquad (3)$$

$$F_s=\epsilon_s\epsilon_0\int_0^\infty dxE(x)^2/2, \qquad (4)$$

where F_0 is the free energy density of the bulk ferroelectric, $E_f=E_f(p=P)$, ϵ_0 is the vacuum permittivity, ϵ_s is the dielectric constant of the semiconductor, $E(x)\equiv E(x,P)$ is the electric field in the semiconductor, $D\equiv D(P)$ is the electric flux (displacement), and l_e is the *effective thickness* of the insulator defined in Eq. (5).

$$l_e=l_d/\epsilon_d, \qquad (5)$$

where ϵ_d is the dielectric constant of the insulator.

Equation (5) can also be used for a multilayered intermediate layer. If the intermediate layer consists of a l_d-thick insulator having ϵ_d and a metal, which means that its overall structure is a ferroelectric/metal/insulator/semiconductor ($F/M/I/S$), Eq. (5) holds. If the intermediate layer consists of a l_{d1}-thick insulator with ϵ_{d1} and a l_{d2}-thick insulator with ϵ_{d2}, Eq. (5) is modified to $l_e=l_{d1}/\epsilon_{d1}+l_{d2}/\epsilon_{d2}$.

For epitaxial thin films, the stress terms is needed,[40] and a total F_f including the stress is

$$F_f=\alpha_1P^2+\alpha_{11}P^4+\alpha_{111}P^6+\eta(\nabla P)^2-\int_0^P dPE_f$$

$$+F_{s1}(\mathbf{S})/2\epsilon_0P^2+F_{s2}(\mathbf{S})$$

$$=[T-(\theta-CF_{s1}(\mathbf{S})]/2\epsilon_0CP^2+\alpha_{11}P^4+\alpha_{111}P^6$$

$$+\eta(\nabla P)^2+\epsilon_0E_f^2(P)/2+F_{s2}(\mathbf{S}), \qquad (2')$$

where $F_{s1}(\mathbf{S})$ and $F_{s2}(\mathbf{S})$ are functions only dependent on the stress tensor ($\mathbf{S}$).[40,41] For c-axis oriented ferroelectric films, Eq. (2′) indicates that *the effect of the stress is to change an effective T_c and the zero point energy* at $P=0$. A numerical analysis using Eq. (2) shows that this effect is relatively small in most cases.[41] Furthermore, it can be minimized by selecting a material and preparation processes.

For $Bi_4Ti_3O_{12}$, F_0 has the following form,[43]

$$F_0=2\alpha_1P_x^2+(2\alpha_{11}+\alpha_{12})P_x^4+2\alpha_{111}P_x^6$$

$$+(\alpha_3+2\alpha_{13}P_x^2)P_z^2+\alpha_{33}P_z^4+\alpha_{333}P_z^6+\alpha_{3333}P_z^8, \qquad (2b)$$

TABLE II. Semiconductor band parameters (see Ref. 45).

	ϵ_s	n_i at 300 K (cm^{-3})	$E_g(0)$ (eV)	γ (eV/K)	γ_2 (K)
Si	11.9	1.45×10^{10}	1.17	4.73×10^{-4}	636
Ge	16	2.4×10^{13}	0.7437	4.774×10^{-4}	235
GaAs	13.1	1.6×10^{6}	1.519	5.405×10^{-4}	204

where P_x is the polarization perpendicular to the c axis, and P_z is along it. The coefficients in Eqs. (2) and (2b) are summarized in Table I.[41–43]

D and $E_s \equiv E(0)$ are related with via Gauss's law at the insulator/semiconductor (I/S) and the ferroelectric/insulator (F/I) boundaries,

$$D = \epsilon_s \epsilon_0 E_s \tag{6a}$$

$$= \epsilon_0 E_f + P\cos\varphi. \tag{6b}$$

If $\nabla P = 0$, there is no net carrier in the ferroelectric. Therefore, using the surface potential $\Psi_s(D) \equiv \Psi(x=0)$, we have an equation for the potential (Fig. 1),

$$l_e D/\epsilon_0 + \Psi_s(D) = -l_f E_f + \delta\phi + V_e, \tag{7}$$

where $\delta\phi$ is the work function difference between the top electrode and the semiconductor, and V_e is the external field. The bottom of the semiconductor is grounded. We incorporated $\delta\phi$ in the theory, following, the scheme used in the metal–oxide–semiconductor device.[44,45]

For a given semiconductor material parameters (Table II), the doping level, and the temperature, the relationship between E_s and Ψ_s is given by solving Poisson equation,[45]

$$-\Delta\Psi(x) = e(N_D^+ - N_A^- + p - n)/\epsilon_s\epsilon_0, \tag{8}$$

where e is the elementary charge, and N_D^+, N_A^-, p, and n are the donor density, the acceptor density, the hole carrier density, and the electron density in the semiconductor, respectively.

Equations (2)–(8) form basic equations in this theory. In the following, a part of them are analytically solved.

Assuming Boltzmann statistics, Eq. (8) is rewritten as,

$$-\Delta\Psi(x) = e(p_0\{\exp[-\beta\Psi(x)] - 1\} - n_0\{\exp[\beta\Psi(x)] - 1\})/\epsilon_s\epsilon_0, \tag{8a}$$

where $\beta = e/kT$, k is the Boltzmann constant, T is the temperature, and p_0 and n_0 are the hole carrier density and the electron density at $x=\infty$, i.e., at $\Psi=0$. In the following argument, $x > 100$ nm can be regarded as ∞, when Ψ_s is an order of 1 V. The intrinsic carrier density n_i, p_0, and n_0 at T are given by[45]

$$p_0 = \{N_A - N_D + [(N_A - N_D)^2 + 4n_i^2]^{1/2}\}/2$$

$$n_0 = n_i^2/p_0$$

$$n_i/n_i(T_0) = (T/T_0)^{3/2}\exp[-E_g/2kT - E_g(T_0)/2kT_0],$$

where E_g is the band gap of the semiconductor at T, and $E_g(T_0)$ and $n_i(T_0)$ are the band gap and the intrinsic carrier density at $T=T_0$, e.g., 300 K, respectively. The temperature dependence of E_g is given by,

$$E_g = E_g(0) - \gamma T^2/(T+\gamma_2),$$

where $E_g(0)$, γ, and γ_2 are known for a given semiconductor material (Table II, Ref. 45).

For one dimensional problem having an infinitely thick semiconductor, the rigorous relation is known,

$$E[\Psi(x)] = \pm(2\{\exp(-\beta\Psi) + \beta\Psi - 1 + [\exp(\beta\Psi) - \beta\Psi - 1]n_0/p_0\})^{1/2}/\beta L_D, \tag{9}$$

with a positive sign for $\Psi > 0$ and a negative sign for $\Psi < 0$, where $\Psi(x)$ is abbreviated as Ψ.[45] The extrinsic Debye length L_D is

$$L_D = (\epsilon_s/ep_0\beta)^{1/2}.$$

Especially, Eq. (9) becomes at $x=0$,

$$E_s = \pm\{\exp(-\beta\Psi_s) + \beta\Psi_s - 1 + [\exp(\beta\Psi_s) - \beta\Psi_s - 1]n_0/p_0\}^{1/2}\sqrt{2}/\beta L_D, \tag{9b}$$

where Ψ_s stands for $\Psi_s(D) = \Psi_s[D(P\cos\varphi)] = \Psi_s(P\cos\varphi)$.

Combining Eq. (7) with Eq. (6b), we have

$$P\cos\varphi = D(1 + l_e/l_f) - \epsilon_0[\delta\phi + V_e - \Psi_s(D)]/l_f. \tag{10}$$

Using Eq. (9), Eq. (4) is rewritten as

$$F_s = \epsilon_s\epsilon_0\int_0^{\Psi_s} d\Psi E(\Psi)/2. \tag{4b}$$

By neglecting the ∇P term, Eq. (1) is reduced to,

$$F = F_0 + \epsilon_s\epsilon_0/2l_f\int_0^{\Psi_s} d\Psi E + D^2 l_e/2l_f\epsilon_0 + \epsilon_0 E_f^2/2 - D\Psi(x = -l_f - l_d)/l_f, \tag{11}$$

$$= F_0 + \epsilon_s\epsilon_0/2l_f\int_0^{\Psi_s} d\Psi E + D^2 l_e/2l_f\epsilon_0 + (\delta\phi + V_e - l_e D/\epsilon_0 - \Psi_s)^2/2l_f^2 - D(\delta\phi + V_e)l_f. \tag{11b}$$

Minimization of Eq. (11) gives an equilibrium P or D under the conditions of Eqs. (6a), (6b), (7), (9), and (9b) for given l_e, l_f, $\delta\phi$, V_e, T, semiconductor material parameters, and GL parameters. [According to Eq. (10), $P=0$ means $D=0$ and $\Psi_s=0$ for $(\delta\phi + V_e)=0$. For $(\delta\phi + V_e)\neq 0$, Eq. (10) needs to be solved using Eq. (9). Equation (10) implies that $P=0$ corresponds to $D = \epsilon_0(\delta\phi + V_e - \Psi_s)/(l_f + l_e)$. For with typical values of $\delta\phi$, l_f, and l_e, e.g., $\delta\phi + V_e \leq 1$ V and $(l_f + l_e) \geq 200$ nm, $D(P=0)$ is less than 0.005 $\mu C/cm^2$, and this corresponds to $\Psi_s(P=0) \leq 0.1$ V through Eq. (9).]

B. Examination of the assumptions

We summarize the related experimental aspects and examine the assumptions.

1. Homogeneous GL theory: $\eta(\nabla P)^2 = 0$

The coefficient η of the ∇P term in the direction of P vector is not experimentally determined or the related phenomena have not yet been confirmed. If η is isotropic, η can be estimated from the 180° or 90° domain wall width ξ, and η is of order of $\xi^2\alpha_1$.[46,47] The typical value of ξ is 0.5–1 nm

for $BaTiO_3$ for the 180° domain wall. Therefore, this term is only important to the total free energy F for a spatial gradient of 1 nm. According to Zhong *et al.*,[8] for a short l_f, the average P should noticeably decrease from the bulk value for one choice of boundary condition, or the surface polarization should noticeably increase from the bulk value for the opposite. By far, its experimental evidences have not yet been reported, especially, in high-quality epitaxial $BaTiO_3$ films of thickness of 10–30 nm.[37] Therefore, we do not include this effect.

As shown in Appendix A of article II, the ∇P effect is equivalent to the change of l_e and l_f to $(l_e+\xi/2)$ and $(l_f-\xi/2)$, and an addition of the energy $(\eta|\nabla P|^2)$. Namely, the ∇P effect is equivalent to an insulating dead layer formation. Therefore, its effect can be included in the present formulation.

2. Boltzmann distribution

A very thin layer of high carrier density $>10^{20}$ cm^{-3} should exist at the semiconductor surface for the accumulation and the strong inversion. In this layer, Fermi–Dirac statistics are appropriate. The thickness of the layer is estimated to be below 1 nm for $\Psi_s \sim \pm 1$ V. Therefore, the resulting changes in the band bending are small, even if the Boltzmann statistics are used.

3. Unidomain

The formation of the multidomain to reduce the electrostatic energy has been commonly discussed as in magnetism.[48] However, this effect would not be dominant in F/S, when the thickness of the space charge layer is much shorter than the lateral dimension of the unidomain (Appendix I).[49]

4. Insulating ferroelectric

The intrinsic carrier density n_i estimated from $E_g \approx 3$ eV indicates $n_i < 10^{-7}$ cm^{-3}. Therefore, we may neglect the effect of free carrier when the depolarization field is small as in F/S structure. Moreover, the field induced carrier generation in ferroelectric is not established, although a space charge layer or a surface layer has been suggested by Känzig and others.[50] If the field effect in ferroelectric is an appropriate assumption, the subsequent results for a finite l_d are only qualitatively correct.

III. APPROXIMATE ANALYTICAL RESULTS AND GUIDING PRINCIPLES

Equation (2) is approximately estimated, using a simplified equation for electric field distribution in the semiconductor for the strong inversion and the accumulation conditions

$$E(x) \approx D/\epsilon_s\epsilon_0(1+x/2d),$$

where $d=\epsilon_s\epsilon_0 D/\beta$.[51] Using this equation, we have

$$\begin{aligned} F \approx & F_0+\beta^{-1}D/l_f+D^2 l_e/2l_f\epsilon_0+\epsilon_0\epsilon_f(\delta\phi-\Psi_s+V_e \\ & -l_eD/\epsilon_0)^2/2l_f^2-D(\delta\phi+V_e)/l_f \\ \approx & F_0+\beta^{-1}D/l_f \\ & +D^2 l_e/2l_f\epsilon_0+\epsilon_0\epsilon_f(\delta\phi+Eg/2+V_e-l_eD/\epsilon_0)^2/2l_f^2 \\ & -D(\delta\phi+V_e)/l_f, \end{aligned}$$

where we estimated Ψ_s as $E_g/2$, and ϵ_f is the relative dielectric constant of ferroelectric which is set to be unity in Sec. II A. We can approximate D as $P\cos\varphi$ under the assumption (4) in a $F/I/S$ structure and obtain for $\varphi \neq 90°$ by setting $V_e=0$,

$$\begin{aligned} F \equiv & F_0+\beta^{-1}P\cos\varphi/l_f+P^2\cos^2\varphi l_e/2l_f\epsilon_0+\epsilon_0\epsilon_f[(\delta\phi \\ & +E_g/2)/l_f-l_eP\cos\varphi/l_f\epsilon_0]^2/2-P\cos\varphi\delta\phi/l_f. \end{aligned} \quad (11c)$$

For a $F/M/I/S$ structure P and D can be independent. The stability in this structure is discussed later.

The first, second, third, and fourth terms represent the bulk free energy, the semiconductor charging, and the insulator polarization, the depolarization, respectively. Typical values of F_0 for $BaTiO_3$, $KNbO_3$, and $PbTiO_3$ are 1, 10, and 70 J/cm^3 at room temperature, respectively, and the values of their P_s are 25, 40, and 75 μC/cm^2, respectively. As shown in the numerical results below, we can approximately use the bulk P_s and the bulk free energy in Eq. (11c). The typical values of both E_g and $\delta\phi$ are 1 V and 0.5, respectively, and β^{-1} is 0.026 V at 25 °C. By substituting these numbers and normalizing l_f by 200 nm and l_e by 0.2 nm, the individual terms in Eq. (11c) (J/cm^{-3}) is estimated for a specific ferroelectric for $\varphi=0°$,

$BaTiO_3$

$$\begin{aligned} & -1+0.03/(l_f/0.2\ \mu\text{m})+3.5(l_e/0.2\ \text{nm})/(l_f/0.2\ \mu\text{m}) \\ & +[0.01/(l_f/0.2\ \mu\text{m})+0.6(l_e/0.2\ \text{nm})/(l_f/0.2\ \mu\text{m})]^2 \\ & \pm 0.7/(l_f/0.2\ \mu\text{m}), \end{aligned}$$

$KNbO_3$

$$\begin{aligned} & -10+0.05/(l_f/0.2\ \mu\text{m})+8.9(l_e/0.2\ \text{nm})/(l_f/0.2\ \mu\text{m}) \\ & +[0.01/(l_f/0.2\ \mu\text{m})+1(l_e/0.2\ \text{nm})/(l_f/0.2\ \mu\text{m})]^2 \\ & \pm 1/(l_f/0.2\ \mu\text{m}), \end{aligned}$$

$PbTiO_3$

$$\begin{aligned} & -70+0.09/(l_f/0.2\ \mu\text{m})+31(l_e/0.2\ \text{nm})/(l_f/0.2\ \mu\text{m}) \\ & +[0.01/(l_f/0.2\ \mu\text{m})+1.8(l_e/0.2\ \text{nm})/(l_f/0.2\ \mu\text{m})]^2 \\ & \pm 2/(l_f/0.2\ \mu\text{m}). \end{aligned} \quad (11d)$$

It should be noted that l_e is an effective length defined by Eq. (5).

The result indicates, that nonzero l_e is the dominant source of the depolarization that is much more intense than usually thought. Second, the instability depends significantly on the ferroelectric material, while it depends only weakly on the semiconductor material and the semiconductor doping concentration. Third, $BaTiO_3$ is the sensitive to the depolarization instability among the three ferroelectrics. Here, we did not include the semiconductor doping concentration dependence entering Eq. (11c) through E_g and $\delta\phi$, while the effect of $\delta\phi$ can be important for a small l_f.

The ferroelectric materials dependence can be summarized by an effective reduction of T_c $(=\theta)$. Using Eqs. (2) and (11c), we have for $\delta\phi=0$

$$\begin{aligned} F \approx & \alpha_1 P^2+\alpha_{11}P^4+\alpha_{111}P^6+\beta^{-1}P\cos\varphi/l_f \\ & +P^2\cos\varphi^2 l_e/2l_f\epsilon_0 \\ & +\epsilon_0(E_g/2l_f-l_eP\cos\varphi/l_f\epsilon_0)^2/2 \\ \approx & \alpha_1 P^2+\alpha_{11}P^4+\alpha_{111}P^6 \\ & +\beta^{-1}P\cos\varphi/l_f+P^2\cos\varphi^2 l_e/2l_f\epsilon_0 \\ & +(P\cos\varphi l_e/l_f)^2/2\epsilon_0-P\cos\varphi E_g l_e/2l_f^2 \\ \approx & [T-\theta+Cl_e(1+l_e/l_f)\cos\varphi^2/l_f+2C\epsilon_0(\beta^{-1} \\ & -E_g l_e/2l_f)\cos\varphi/Pl_f]P^2/2C\epsilon_0+\alpha_{11}P^4+\alpha_{111}P^6 \end{aligned} \tag{12a}$$

$$\approx (T-\theta+Cl_e/l_f\cos\varphi^2)P^2/2\epsilon_0 C+\alpha_{11}P^4+\alpha_{111}P^6. \tag{12b}$$

Equation (12b) is sufficient for a small l_e/l_f, while Eq. (12a) is needed for large l_e/l_f and E_g. For $KNbO_3$ and $PbTiO_3$, the maximum l_e/l_f of that allows P_s near 0 °C is given by

$$(l_e/l_f)_{\max}=\theta/(C\cos\varphi^2). \tag{13}$$

Ferroelectric material having a *low thermodynamic linear susceptibility suppresses the depolarization instability*, and for $\varphi=0°$, the $(l_e/l_f)_{\max}$ is 0.002 for $KNbO_3$ and 0.003 for $PbTiO_3$. The epitaxial stress effect discussed in Eq. (2) can increase θ by 100–200 °C and increase the maximum l_e/l_f by 20%–50%. Equation (13) also predicts that *the depolarization instability due to the insulating buffer layer is suppressed by increasing φ for an insulating ferroelectric*. However, the coercive field is increased by a factor of $\cos\varphi^{-1}$ and the switching voltage is expected to increase proportionally.

For $l_e=0$, we have from Eq. (11c), $F\approx F_0+\beta^{-1}P/l_f+\epsilon_f\epsilon_0(\delta\phi+E_g/2)^2/2l_f^2-P\cos\varphi\delta\phi/l_f$. For $l_e=0$, a polarity-, a work function-, and an ϵ_f-dependences becomes evident, especially at a short l_f.

In general, P_s can be more stable in one polarity and less stable in the other, if the semiconductor is doped or $\delta\phi$ is finite. This is expressed by considering more precise expression of Ψ_s in Eq. (11c) instead of $\Psi_s\approx E_g$. Namely, we have $\Psi_s=E_g+\delta$ for one polarity and $\Psi_s=E_g-\delta$ for the opposite, when one carrier type is dominant in a semiconductor by doping. Equation (11c) suggests that this asymmetry, i.e., an instability of one polarity, can be removed by choosing a metal electrode having an appropriate work function, if the effect of defects at the interface is negligibly small. Alternatively, a large $\delta\phi$ can stabilize one polarity of ferroelectric phase for short l_f.

IV. NUMERICAL RESULTS

We solve Eq. (11b) numerically for $\varphi=0$ (Figs. 2–10, 13 and 15). For $\varphi\neq0$ with $\delta\phi=0$, the minimum l_f for the existence of ferroelectric polarization or the maximum l_e/l_f is obtained approximately, multiplying the minimum l_f by $\cos\varphi^2$ or dividing and the maximum l_e/l_f by $\cos\varphi^2$.

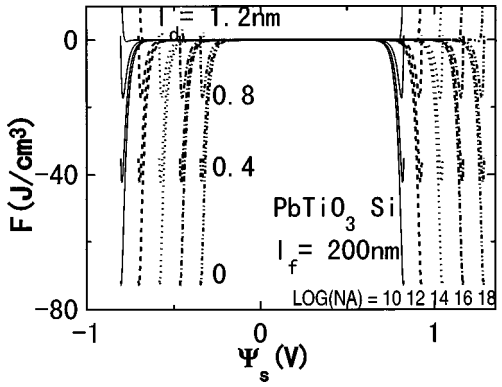

FIG. 2. Total free energy F to induce the semiconductor surface potential Ψ_s at 25 °C for $l_f=200$ nm, $l_d=0$, 0.4, 0.8, 1.2 nm in $PbTiO_3/SiO_2/Si$ at 25 °C. $N_A=10^{10}$ (—), 10^{12} (---), 10^{14} (....), 10^{16} cm^{-3} (_._._), and 10^{18} cm^{-3} (_.._.._).

A. $PbTiO_3$

First, the result for a c-axis oriented $PbTiO_3$/insulator/Si is shown with $N_D=0$, where the insulator is SiO_2 having $\epsilon_d=3.9$, i.e., $l_e=l_d/3.9$. The typical value of $\delta\phi$ ranges from -1 to 1 eV, and its effect was found to be small, especially, for $PbTiO_3$ with thickness >100 nm. Therefore, we set $\delta\phi+V_e$ to be zero in the following calculation except Fig. 7.

Figure 2 shows the free energy F to induce the semiconductor surface potential Ψ_s, while each line corresponds to different values of l_d and N_A. Each line has well-defined double minima, indicating the bistability, and shifts parallel as N_A increases. For $l_d<1.2$ nm, the F minima increase with l_d, where $l_d=0.4$ nm corresponds to one atomic layer. For $l_d=0$, the values of the electric flux D at the minima are similar to the bulk value 75 $\mu C\,cm^{-2}$. Furthermore, the depolarization field, i.e., the field in ferroelectric E_f is well below the coercive field 100 kV cm^{-1} as seen in Fig. 3.

Hence, the *unidomain in this F/S structure should be stable*, allowing a sufficiently large domain size and Ψ_s to induce the conductance modulation. Indeed, 10 month retention of conductance modulation by ferroelectric field effect was recently reported.[32] This conclusion is different from that made by Batra and colleagues,[14,15] but the difference is mainly due to that of the ferroelectric materials and to the explanation of the calculated results. For $l_d\neq0$, E_f is much higher than the coercive field, although it has negative F minima for $l_d<0.9$ nm.

Figure 4 shows the temperature (T) dependence of F, D, Ψ_s, and E_f for the three sets of l_d and l_f: (1) $l_d=0$ and $l_f=200$ nm; (2) $l_d=0$ and $l_f=5$ nm; (3) $l_d=0.9$ and $l_f=200$ nm. There are six different lines in each set that correspond to the positive and the negative polarities for the three different N_A. However, they can be only distinguished in Figs. 4(c) and 4(d), and, e.g., a large polarity and N_A dependence is seen for the set (2), in accordance with Eqs. (11c) and (11d). The lines of sets (3) and (1) are identical, if one of them is shifted along abscissa. Namely their only difference is T_c, as discussed Sec. III.

Both short l_f and nonzero l_d reduce the transition temperature and the absolute value of F. Especially, the effect of l_d is significant. The transition temperature is reduced by the

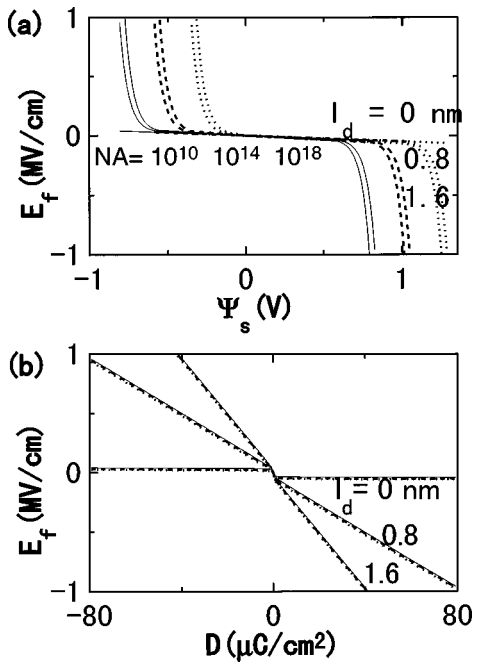

FIG. 3. Field in ferroelectric E_f vs Ψ_s (a) and E_f vs the net space charge per area D (b) for $l_f=200$ nm and $l_d=0$, 0.8, 1.6 nm in $PbTiO_3/SiO_2/Si$ at 25 °C. $N_A=10^{10}$ cm^{-3} (—), 10^{14} cm^{-3} (---), and 10^{18}cm^{-1}(....).

same order of magnitude as estimated in Eq. (12b), i.e., $Cl_d/l_f \approx 200$ K, although it is severer. These results are summarized in terms of the transition temperature reduction in Fig. 5. The enhancement of E_f by the nonzero l_d and the short l_f is evident in Fig. 4(c). On the other hand, D near room temperature (RT) (25 °C) is insensitive to l_d and l_f. This allows the approximation used in Eq. (11d). The slight increases of E_f and Ψ_s with T in Figs. 4(c) and 4(d) are caused by the Boltzmann factor in Eq. (8a).

The phase transition sharpens for a short l_f with $l_d=0$ as shown in the set (2) in Fig. 4(b). This agrees with the theoretical result by Batra *et al.*[14] that the semiconductor electrode changes the second order phase transition of triglycine-sulfate (TGS) into the first order. Contrarily, a nonzero l_d mildens the change at the first-order phase transition.

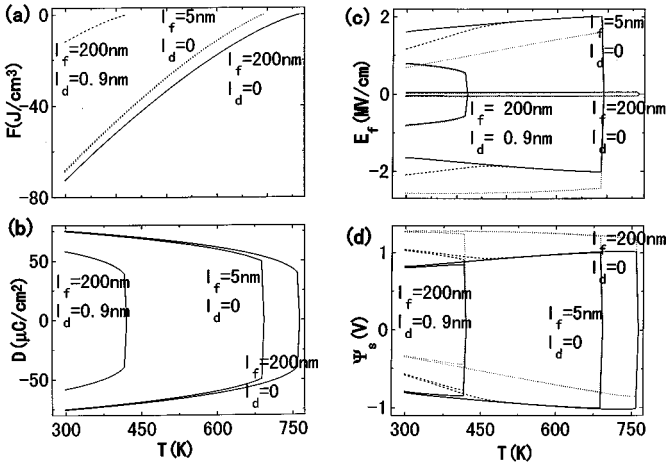

FIG. 4. Temperature dependence of F (a), D (b), E_f (c), and Ψ_s (d) for three sets of l_d and l_f: (1) $l_d=0$ and $l_f=200$ nm, (2) $l_d=0$ and $l_f=5$ nm, (3) $l_d=0.9$ and $l_f=200$ nm in $PbTiO_3/SiO_2/Si$. Three different lines in each set correspond to the positive and the negative D for $N_A=10^{10}$ cm^{-3} (—), 10^{14} cm^{-3} (---), and 10^{18} $^{-3}$ (.....).

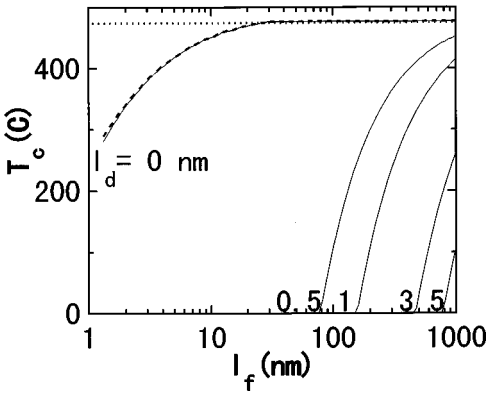

FIG. 5. Effective T_c of $PbTiO_3$ in $PbTiO_3/SiO_2/Si$ for $l_d=0$, 0.5, 1, 3, 5 nm and $N_A=n_i$ (—), and 10^{18} cm^{-3} (----). The difference of T_c for two N_A values are too small to be distinguished except those for $l_d=0$ at short l_f.

Figures 6(a) and 6(b) show l_f-dependence of D and F, which is regarded as a thickness-induced phase transition. For $l_d=0$, the ferroelectric phase is stable even at $l_f=1$ nm, while a polarity dependence at a high N_A becomes evident as l_f decreases. On the other hand, it is unstable below $l_f=1$ μm, if the SiO_2 thickness (l_d) exceeds 5 nm, i.e., $l_e=1.3$ nm. A nonzero l_d mildens the change at the size-induced phase transition as seen in Fig. 6, which is consistent with the T-induced phase transition in Fig. 4(a). For $l_d=3$ nm the minimum l_f for stable ferroelectric polarization is $\sim$500 nm for $\varphi=0°$ as seen in Fig. 6(a), which means the minimum l_f is $\sim$120 nm for $\varphi=60°$.

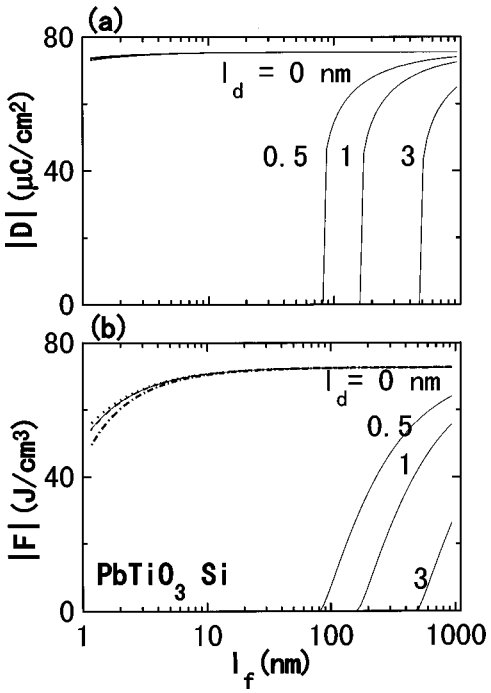

FIG. 6. Thickness (l_f)-dependence of $|D|$ (a) and $|F|$ (b) for $l_d=0$, 0.5, 1, 3 nm and $N_A=n_i$ (—) and $N_A=10^{18}$ cm^{-3} (.....: $D<0$, ._._._.: $D>0$) in $PbTiO_3/SiO_2/Si$ at 25 °C.

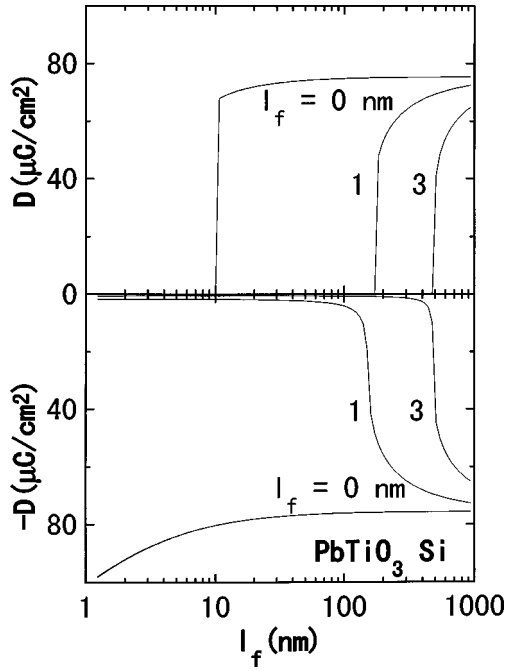

FIG. 7. Thickness (l_f)-dependence of D for $l_d=0$, 1, 3 nm and $\delta\phi=-1$ eV in $PbTiO_3/SiO_2/Si$ at 25 °C. The curves for $N_A=n_i$ at 10^{18} cm^{-3} are plotted but are indistinguishable to each other.

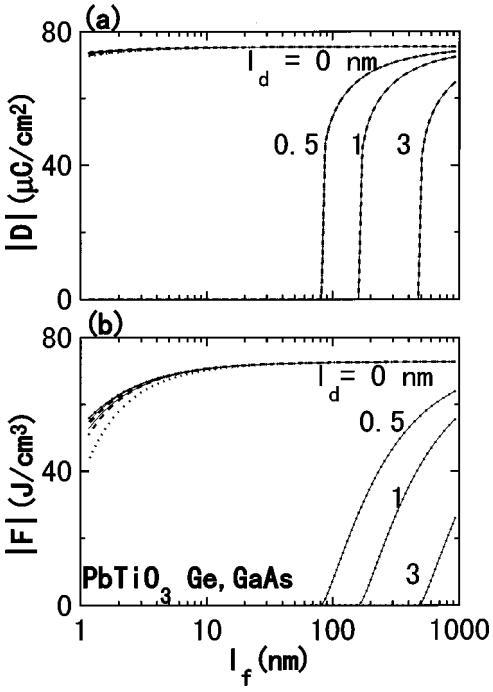

FIG. 8. Thickness (l_f)-dependence of $|D|$ (a) and $|F|$ (b) in $PbTiO_3/SiO_2/Ge$ [$N_A=n_i$ and 10^{18} cm^{-3} (—)] and for $PbTiO_3/SiO_2$/GaAs [$N_A\approx n_i$ (----) and $N_A=10^{18}$ cm^{-3} (.....)] with $l_d=0$, 0.5, 1, 3 nm for at 25 °C.

Figure 7 is a plot similar to Fig. 6(a) with $\delta\phi=-1$ eV. Large work function deference modify the stability and makes the polarization monostable at a short l_f. The small D below 100 nm for $D<0$ and $l_d\neq 0$ is primarily determined by the balance of the third and the last terms in Eq. (11). Namely, the minimization of these terms ($D^2 l_e/2l_f\epsilon_0 - D\delta\phi/l_f$) yields $D=\epsilon_0\delta\phi/l_e$, while the values in Fig. 7 are approximately a half of this number. We may say that D in this region is not caused by a real ferroelectricity because of $P\ll$ *a* bulk P_s.

Similar result were obtained by substituting Si with Ge or GaAs as shown in Fig. 8. F in $PbTiO_3/SiO_2$/GaAs with $N_A=10^{18}$ cm^{-3} (dotted line) is evidently smaller for $D>0$ than for $D<0$ below $l_f=10$ nm. The effect of semiconductor material on the size effect, where the dominant controlling factor is the band gap, is small, especially for $l_d\neq 0$. This is also in agreement with the analysis in Sec. III. Additionally, the minimum l_f for $l_d=0$ can be shorter than the value shown in Fig. 6, if we use $\epsilon_f>1$.

B. Other ferroelectric and the material dependence

The stability in the ferroelectric/SiO_2/Si with $N_D=0$ is examined for other ferroelectric materials. Figure 9 shows l_f-dependence of D in $BaTiO_3$ and $KNbO_3$ structures. The overall l_f-dependence is qualitatively same as that for $PbTiO_3$, although the minimum l_f for $D\neq 0$ depends strongly on the ferroelectric material.

The ferroelectric material dependence can be characterized as the l_d-dependence of the minimum l_f that allows a nonzero P_s. Figure 10 shows the result for ferroelectric/SiO_2/Si at 25 °C, where ferroelectrics are $BaTiO_3$, $KNbO_3$, and $PbTiO_3$. The linear relation between l_f and l_d is evident, which agrees with Eq. (13). Its inclinations divided by ϵ_d, i.e., the maximum $l_e/l_f(=l_d/\epsilon_d l_f)$, are 0.001 and 0.0016 for $KNbO_3$ and $PbTiO_3$, respectively. These values are approximately halves estimated by Eq. (13).

P_s of $Bi_4Ti_3O_{12}$ has three components: $50/\sqrt{2}$ μC cm^{-2} along the *a* axis, $50/\sqrt{2}$ μC cm^{-2} along the *b* axis, and 4 μC cm^{-2} along the *c* axis. Examining Eqs. (11c) and (11d), we expect that an *a*- or *b*-axis oriented $Bi_4Ti_3O_{12}$ has behaviors similar to $KNbO_3$ and $PbTiO_3$. However, a *c*-axis oriented $Bi_4Ti_3O_{12}$ should behave differently, because it allows a high D in plane and a low D out of plane simultaneously. Additionally, P_s of 4 μC cm^{-2} is more than sufficient for the field effect modulation of the Si conductance.

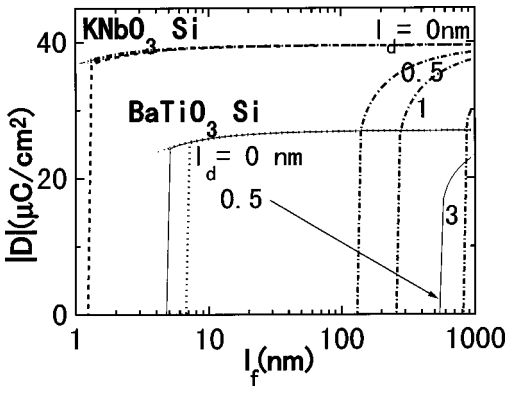

FIG. 9. Thickness (l_f)-dependence of D for $BaTiO_3/SiO_2$/Si [—:$N_A\approx n_i$ ($D<0$, $D>0$) and $N_A=10^{18}$ cm^{-3} ($D<0$), ...: $N_A=10^{18}$ cm^{-3} ($D>0$)] and for $KNbO_3/SiO_2$/Si [._._._.: $N_A\approx n_i$ ($D<0$, $D>0$) and $N_A=10^{18}$ cm^{-3} ($D<0$), ----: $N_A=10^{18}$ cm^{-3} ($D>0$)] at 25 °C. The values of l_d are 0 and 0.5 nm for $BaTiO_3/SiO_2$/Si and 0, 0.5, 1, 3 nm for $KNbO_3/SiO_2$/Si.

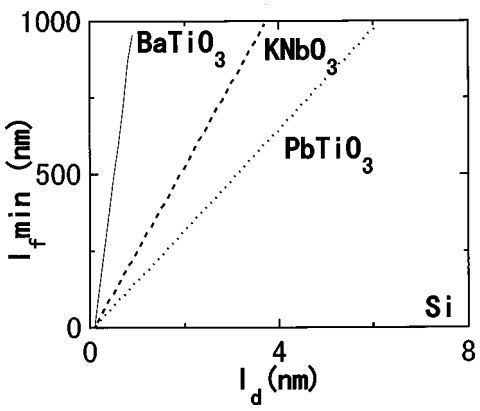

FIG. 10. Dependence of the minimum l_f on l_d in ferroelectric/SiO_2/Si at 25 °C for $N_A \approx n_i$ and 10^{18} cm^{-3}, where ferroelectrics are $BaTiO_3$ (—), $KNbO_3$ (---), and $PbTiO_3$ (.....).

Figures 11(a) and 11(b) show the dependence of F on D and Ψ_s in c-axis oriented $Bi_4Ti_3O_{12}/SiO_2/Si$, respectively. Unlike those in $BaTiO_3$, $KNbO_3$, and $PbTiO_3$, P_s can exist for $l_d \geqslant 10$ nm. However, P_s along the c axis vanishes for $l_d > 1$ nm.

V. MULTIDOMAIN EFFECT

The above results demonstrated that a unidomain homogeneous insulating ferroelectric phase cannot exist in $F/I/S$, if there are no surface states at the ferroelectric/insulator interface. The assumptions of Boltzmann distribution and $\nabla P = 0$ are unlikely to cause a significant error in estimation of the stability. Stabilization of the ferroelectric phase by the multidomain formation has frequently been discussed. In oriented thin films, no loop domain configuration has been experimentally observed. Therefore, we consider only 180° domain walls.

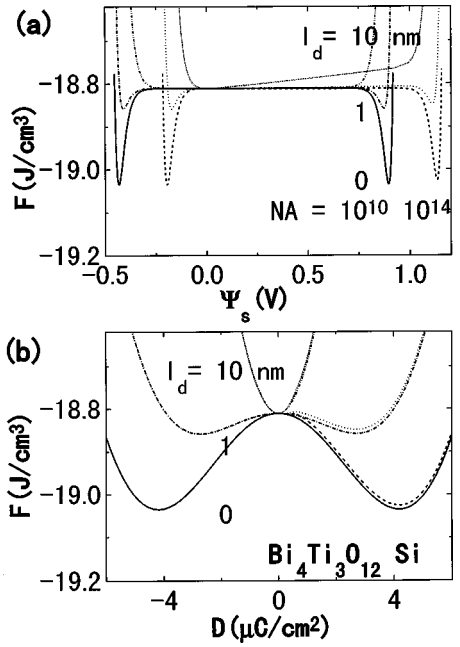

FIG. 11. Dependence of F on D (a) and Ψ_s (b) in c-axis oriented $Bi_4Ti_3O_{12}/SiO_2$/ at 25 °C. Different lines (—), (---), (_._._.), (...), (_.._.._), and (.....) correspond to $l_d = 0$ and $N_A = 10^{12}$ and 10^{14} cm^{-3}, $l_d = 1$ nm and $N_A = 10^{12}$ and 10^{14} cm^{-3}, $l_d = 10$ nm and $N_A = 10^{12}$ and 10^{14} cm^{-3}.

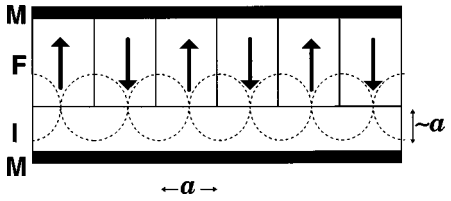

FIG. 12. Multidomain configuration in $F/I/M$ as model to estimate stability of ferroelectric phase in $F/I/S$. Dashed lines indicate the electric field lines.

We model $F/I/S$ as $F/I/M$, by neglecting the effect of the semiconductor charging energy, because it is much smaller than the insulator charging energy. Therefore, the results below give an upper limit of the stabilization by the multidomain effect. The model is shown in Fig. 12, where $\mathbf{P}(y) = P\mathbf{x}$ for $2an < y < (2n+1)a$ and $\mathbf{P}(y) = -P\mathbf{x}$ for $(2n+1)a < y < 2a(n+1)$ ($\mathbf{x}$: unit vector in the x direction, n: integer). This configuration corresponds to the net $D = 0$, while the free energy F should have a higher energy for the net $D \neq 0$. F is given by

$$F_f = F_0 + \eta(\nabla P)^2 + F_d = F_0 + F_w + F_{d1} + F_{d2},$$

where F_w is the excess energy due to domain formation given in Appendix II.

Depolarization energies F_{d1} and F_{d2} are given by,

$$F_{d1} = \int_0^{2a} dy \int_0^{l_f} dx [\nabla \Psi(x,y)]^2 / 2a l_f$$

$$= 2Pa \left(\sum{}' \, n^{-3} r_n \sinh n\kappa l_f \sinh n\kappa l_d \right) \Big/ \, \pi \epsilon_0 l_f, \tag{14a}$$

$$F_{d2} = \epsilon_d \epsilon_0 \int_0^{2a} dy \int_{l_f}^{l_f + l_d} dx [\nabla \Psi(x,y)]^2 / 2a l_f$$

$$= \pi a \left(\sum{}' \, n^{-3} r_n^2 \epsilon_d \sinh^2 n\kappa l_f \sinh 2n\kappa l_d \right) \Big/ \, \epsilon_0 l_f, \tag{14b}$$

where Σ' means the sum $n = 2m+1$ ($m = 1,2,...,\infty$), and κ and r_n are given in Appendix II. Substituting these expressions for F_{d1} and F_{d2}, we minimize the F with respect to P and a for given l_f and l_d.

F_d and F_w are rewritten as $F_d = c_d P^2 / 2\epsilon_0$ and $F_w = c_w P^2 / 2\epsilon_0$, where c_d and c_w are constants determined by ϵ_d, a, l_d, and l_f. Using these formulas *the effect of depolarization in multidomain and the domain wall formation is completely expressed as an effective T_c reduction δT*,

$$F = [T - (\theta - \delta T)] P^2 / 2\epsilon_0 C + \alpha_{11} P^4 + \alpha_{111} P^6,$$

where $\delta T = C c_d + C c_w$. A low *linear susceptibility suppresses the depolarization instability* as suggested before. The minimization of F with respect to a is equivalent to that of the effective T_c reduction δT.

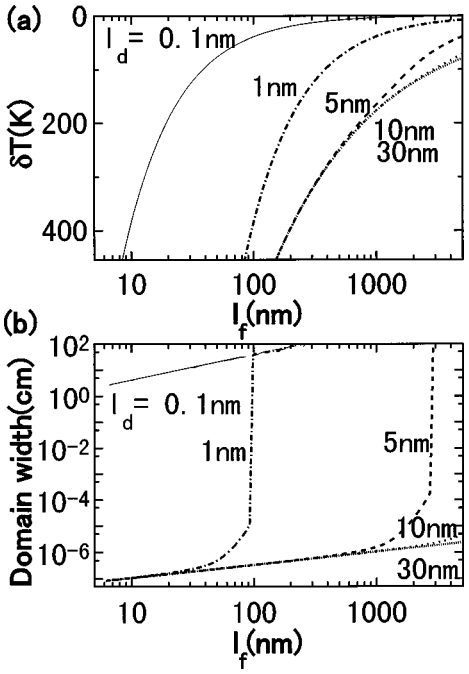

FIG. 13. Numerically calculated T_c reduction and the domain size a where the total electric free energy is minimized in the configuration shown in Fig. 12.

Using the asymptotic forms, we have approximately $F_d = F_{d1} + F_{d2} \approx P^2 a/2\pi^3 \epsilon_0 (\epsilon_d + l) l_f$. Combing $F_w = 8\eta P^2/3\xi a$, approximate analytical expressions of a at the minimum effective T_c reduction and the minimum δT for $a \sim l_f$ and $a > l_d$ are

$$a = 4[\pi^3 \eta \epsilon_0 (\epsilon_d + l) l_f / 3\xi]^{1/2}, \tag{15a}$$

$$\delta T = 8C[\epsilon_0 \eta / 3\pi^3 \xi (\epsilon_d + 1) l_f]^{1/2}. \tag{15b}$$

Estimating η as in Appendix II, a is 7 nm $(l_f/200\ \text{nm})^{1/2}$ for $PbTiO_3$ and 3 nm $(l_f/200\ \text{nm})^{1/2}$ for $BaTiO_3$, where we use $\epsilon_d = 3.9$ and $\xi = 0.9$ nm. For same parameters, δT is estimated to be 130 °C $(200\ \text{nm}/l_f)^{1/2}$ for $PbTiO_3$. These estimations well account for the l_f-dependence and the values in the numerical results for $l_d \geqslant 5$ nm.

Figure 13 shows the numerical results for the l_f-dependence of a and δT for $PbTiO_3$ with $\epsilon_d = 3.9$. We approximated ξ as a constant (0.9 nm), because only a small change of ξ by l_f was found. The ferroelectric phase exist for $\delta T \leqslant 450$ °C at RT. We can virtually regard the ferroelectric as unidomain, if a satisfies $a \gg l_f$.

In ferroelectric thin films, the major effect of the multidomain formation is to confine the electric flux near the ferroelectric surface region with thickness of a in the ferroelectric and in the insulator, as illustrated in Fig. 12. For $F/I/M$ (and also $F/I/S$), this means the reduction of the depolarization (F_{d1}) and the insulator charging energies (F_{d2}) by a factor of a/l_d. Therefore, the reduction of electrostatic energy by this mechanism is effective only for $a < l_d$. Indeed, a multidomain state is stable for $a < l_d$ in Fig. 13(a). For example, F_d for a multidomain is reduced to one tenth of that for unidomain, for a relatively thick l_d of 30 nm.

The thickness limit given by $(\theta - \delta T) \approx 25$ °C, i.e., $\delta T \approx 450$ °C in Fig. 13(a) is a lower limit and is 150 nm for

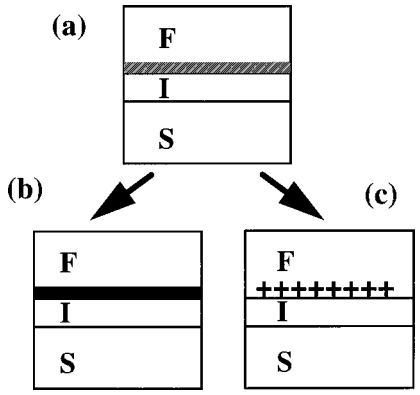

FIG. 14. Classification of the effect of disorder at the ferroelectric/insulator interface in $F/I/S$. $F/I/S$ having the disorder layer formed through reaction, which is denoted by the gray area in (a), is effectively modeled as (b) and (c). The dark area and + represent conductive layer (b) and charged trap or defect (c), respectively.

$PbTiO_3$ with $l_d \geqslant 5$ nm even for the net $D = 0$. On the other hand, c-axis oriented *ferroelectric-phase* films having thickness 100 nm or less are experimentally observed, suggesting that the multidomain effect alone is insufficient to stabilize ferroelectric phase in $F/I/S$.

VI. DISCUSSION: INTERFACIAL DEFECTS, THERMODYNAMIC, NONTHERMODYNAMIC, AND PREPARATION-LIMITED INSTABILITIES

We have shown the depolarization instability in Secs. III and IV. To compare these results with experimental, we first examine other instabilities.

The thermodynamic depolarization instability is expected to change the crystallographic and the electrical properties of the ferroelectric. It changes also the space charge layer in the semiconductor surface. However, there are various *extraneous* mechanisms destabilizing the space charge layer that are structure dependent. We define the instability as an extraneous, when it can be removed by improving the material and the interface properties. A nonthermodynamic instability is defined, when the space charge layer disappears without extraneous instabilities but P_s is stable. The disorders and the defects, or the surface states, at the interfaces change the stability drastically from an ideal case and can destabilize and stabilize the ferroelectric phase and the space charge layer. Therefore, we first summarize the effects of disorders and defects, and then, the mechanisms of the instability are examined for specific structures: Sec. VI B F/S, Sec. VI C $F/I/S$, and Sec. VI D $F/M/I/S$. (All the structures for ferroelectric FET belong to one of these three structures.)

A. Effect of the disorders and the defects at the interface

In real ferroelectric thin-film heterostructures, a significant amount of disorders and defects exist at the interface of F/S, F/I in $F/I/S$, and F/M and M/I in $F/M/I/S$ [Fig. 14(a)]. They effectively change the stability when they exist in the F/S and the F/I interfaces. They can be classified into two groups: the formation of semimetallic or semiconducting layer at the interface [case A, Fig. 14(b)] and the formation

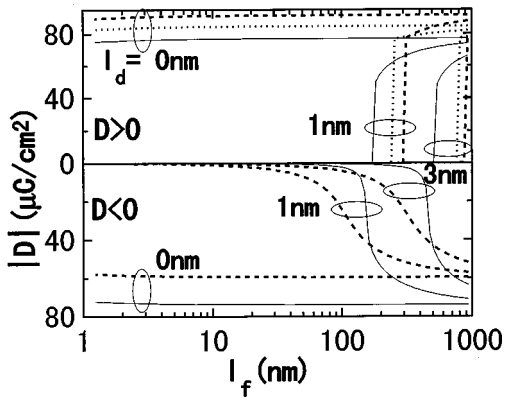

FIG. 15. Thickness (l_f)-dependence of $|D|$ for l_d=0,1, 3 nm and N_A $=10^{14}$ cm^{-3} in $PbTiO_3/SiO_2/Si$ at 25 °C having positively charged defects at the ferroelectric/insulator. The sheet carrier density S due to the defects is 10^{13} cm^{-2} (—), 10^{14} cm^{-2} (-----), and 10^{15} cm^{-2} (.....).

of charged layer at the interface while keeping the insulating nature of the insulator and the ferroelectric [case B, Fig. 14(c)].

In case A, the carriers are contained at the interface and are free to move in the interfacial layer. Therefore, $F/I/S$ and F/S structures becomes effectively $F/M/I/S$ and ferroelectric/metal/semiconductor ($F/M/S$), respectively. The stability in $F/M/I/S$ is discussed in Sec. VI D. P_s in a sufficiently large unidomain in $F/M/S$ is bistable, but practically no conductance modulation should be observed.

In case B, the interface is not severely damaged as in case A and still retains insulating properties. Namely, we assume fixed charges at the interface and no carrier conduction in the interface. In such a situation, we can estimate the stability by modifying Eq. (6b) for $\varphi=0$ into

$$D=\epsilon_0 E_f+P+qS, \tag{6c}$$

where S and q are the sheet charge number density and the charge of the defect, respectively. The effect of S is to stabilize P_s in one polarity and destabilize it in the other. If $qS\approx -P$, $D\approx 0$, and P_s are monostable and free from the depolarization instability.

Figure 15 shows the thickness dependence of D for typical values of S in $PbTiO_3/SiO_2/Si$. We assumed q to be $+e$, because the acceptor type traps, e.g., traps due to oxygen vacancy, are reported for many ferroelectric thin films. The values of S are 10^{13}, 10^{14}, and 10^{15} cm^{-2}, which correspond approximately to $0.02|P_0|$, $0.2|P_0|$, and $2|P_0|$, where $|P_0|$ is the absolute value of P_s in the bulk $PbTiO_3$. For $eS<|P_0|$, the minimum thickness l_f for a given l_d which allows ferroelectric phase is shorter for $D<0$ than for $D>0$. For $eS>|P_0|$ and $D<0$, ferroelectric phase is totally unstable. Here, the equilibrium P is negative for $eS>|P_0|$ and $D>0$. Negative D values, which are two order of magnitude smaller than bulk value ($\approx|P_0|-eS$), are found to exist for $eS=0.02|P_0|$ and $0.2|P_0|$. This was unexpected from simplified analytical calculation, and the D value of $0.1-1$ μC/cm^2 agrees with the experimentally estimated semiconductor surface charge in $F/I/S$ structures.[27,29]

The charged defects or traps can be formed before and after the polarization switching. Even for D reduced to one hundredth of the bulk P, an enormous field exists in the insulator of $F/I/S$ for a finite l_d, as inferred from Fig. 3. This field should increase the charged trap density at the interface and finally compensate P, i.e., extinguish the conductance modulation with time.

B. *F/S*

First, we survey extraneous mechanisms. It is extraordinarily difficult to create this structure without forming an intermediate layer between the ferroelectric and the semiconductor, especially when an oxide ferroelectric is used in combination with the conventional semiconductor materials. Such a layer is usually disordered and grown through the chemical reaction or the interdiffusion of these materials.

As discussed in Sec. VI A, *a unidomain ferroelectric is monostable* in case B, and the switching properties should be suppressed. This is because the disordered layer is usually a heavily p- or n-doped semiconductor having a low carrier mobility. The layer acts also as a carrier trap, and the space charge in the semiconductor created by the ferroelectric polarization is also trapped. As the traps are filled with time, the conductance modulation should decrease with time, although ferroelectric is stable. In the most severe case, i.e., case A, no conduction modulation is observed. There are several experiments of the conductance modulation showing the polarity-dependence opposite to the ferroelectric field effect,[23,30] usually called as ''injection dominated.''

The conductivity modulation of F/S using a *bulk* ferroelectric like TGS[17–20,22] or $BaTiO_3$ (Ref. 21) single crystals has been reported by many authors. The present study suggests no depolarization instability. Indeed, one of them succeeded to retain the conductance modulation more than a few hours. In these experiments, the interface between the ferroelectric crystals and semiconducting film seems still to be disordered, which have likely limited the retention.

Experiments on the depolarization instability in a TGS film on a Si crystal are performed by Batra *et al.* They observed asymmetric polarization hystereses and attributed it to the depolarization instability.[15,16] However, similar experiments on SiO_2/Si by us demonstrated that the asymmetric hysteresis was due to a p/n junction formation in the semiconductor inversion layer.[52] Moreover, we have found no asymmetric hystereses in (Pb,La)(Ti,Zr)O_3/p-type La_2CuO_4 and in (Pb,La)(Ti,Zr)O_3/n-type $SrTiO_3$.[53] In this experiment, p-type La_2CuO_4 and n-type $SrTiO_3$ are heavily doped semiconductors. According to the depolarization instability, a heavy doping should have enhanced the asymmetry, which is contrary to the experimental results. We can naturally explain the absence of the asymmetry by the p/n junction width, because the p/n junction width is significantly reduced for heavily doped semiconductors. Therefore, their experiments seem to be insufficient to prove the depolarization instability.

Moreover, the conductance modulation of La_2CuO_4 in 350-nm-thick (Pb,La)(Ti,Zr)O_3/La_2CuO_4 was unchanged for one day[31] and retained its half value after 10 months in air.[32] These results demonstrate that F/S structures can have a stable P_s and a stable conductance modulation, in agreement with the present theory.

We should note that P_s in TGS/CdS should be categorized into ''metastable,'' according to Batra *et al.* From practical viewpoint, we conclude that its P_s is stable.

There have been attempts to grow an oxide ferroelectric directly on Si structure. However, all the results, e.g., the results in Refs. 23, 25, and 26, and the recent results, indicate an existence of an intermediate layer, to our best knowledge. In agreement with the above discussion, the conductance modulation was reported to die in a few minutes, or in the best case, in a day, as long as the life time of the conductance modulation was stated in the article. We should remind us that P_s should still be retained in this case.

C. *F/I/S*

First, we survey extraneous mechanisms. As long as ferroelectric has a chemically right structure, and SiO_2 is used as an insulator adjacent to semiconductor, this structure can reduce preparation-limited depolarization instability. One mechanism often pointed out is the series capacitance of the insulator layer. This causes an insufficient bias field across the ferroelectric when the external bias is applied to reverse the polarization. Most engineers consider it as the main mechanisms of the short retention of the conductance modulation in $F/I/S$ and $F/M/I/S$.

However, a large field $D/\epsilon_d\epsilon_0$, e.g., 3 MV cm^{-1} for $D=1\ \mu$C cm^{-2}, exists in the insulator and an enormous depolarization field in ferroelectric (Fig. 3). These fields would increase the trap-filling and the defect formation at F/I interface. As shown in Sec. VI A, *P_s is stable, but* the conductance modulation can be unstable, if the insulator is not perfect. In such cases, the final state of the $F/I/S$ should be regarded as $F/M/I/S$.

All the experiments exhibit a fast decay of the conductance modulation which is likely related with the trap as discussed above,[27–29] except the for one by Sugibuchi *et al.*[24] However, many $F/I/S$'s (S=Si) show well-defined capacitance voltage hystereses suggesting an existence of a single-domainlike configuration. For typical l_d and ϵ_d, they are difficult to explain by the present theory without heavy disorder at the F/I interface.

Sugibuchi *et al.* achieved the longest retention of conductance modulation among the results that used the conventional semiconductors like Si, Ge, and GaAs. They used $Bi_4Ti_3O_{12}$ as a ferroelectric. However, $Bi_4Ti_3O_{12}$ has little advantage as compared with other ferroelectric oxides in view of the thermodynamic depolarization instability (Fig. 11). This issue is difficult to explain by the present theory and is discussed in article II.

D. *F/M/I/S*

First, we survey extraneous mechanisms. For a unidomain ferroelectric, the situation is identical to that in $F/I/S$. However, only two domains having a positive and a negative polarization are sufficient to extinguish a net D in the insulator and the semiconductor, practically without no restriction on the domain size. Therefore, D should diminish until E_f becomes less than the coercive field, by changing the domain configuration. For typical parameters, E_f is estimated to be

$$150\ \text{kV cm}^{-1}(D/1\ \mu\text{C cm}^{-2})(l_d/10\ \text{nm})/(l_f/200\ \text{nm})/$$
$$(\epsilon_d/3.9)+50\ \text{kV cm}^{-1}(\Psi_s/1\ \text{V})/(l_f/200\ \text{nm})$$
$$\pm 50\ \text{kV cm}^{-1}(\delta\phi/1\ \text{V})/(l_f/200\ \text{nm}).$$

The coercive field can be tuned to exceed this value of E_f. This means that both P_s and conductance modulation can be stable, if the insulator can endure a high electric field $D/\epsilon_d\epsilon_0$ estimated in Sec. VI B. One should note that F is negative and approximately equal to the bulk GL energy F_0 only for a net $D\approx 0$, unlike in $F/I/S$.

However, the free carrier can flow into the metallic electrode on the insulator through the ferroelectric, if it has a finite conductivity. This carrier compensate the net ferroelectric charge and extinguish the conductance modulation. The leakage current I_L of well-controlled ferroelectric film is $\sim 10^{-9}$ A cm^{-2}. The retention time should be the time constant $D/I_L \approx 10^3$ s for $D=1\ \mu$C cm^{-2}, if the top electrode is grounded.

Experimentally, the initial net charge of the space layer D was typically 1 μC cm^{-2} that was retained for less than 1 h.[28] D can be explained by assuming a coercive field of 200 kV cm^{-1}, and the retention time agrees with the estimate based on the resistivity. The change of the conductance modulation is modeled as that of D,

$$dD=-R(E_f)E_f dt\approx -R(Dl_e/\epsilon_0 l_f)Dl_e/\epsilon_0 l_f dt,$$

where R is the resistivity of the ferroelectric. If $R=a_1E_f^n$, the equation implies

$$D\propto \exp(-Rl_e t/\epsilon_0 l_f) \quad \text{for } n=0 \quad \text{and}$$
$$D\propto [a_2+na_1(l_e/\epsilon_0 l_f)^{n+1}t]^{-1/n}\propto t^{-1/n} \quad \text{for } n>0,$$

where a_1 and a_2 are constants.

VII. CONCLUSION

We estimated the stability of P_s and the space charges layer in a semiconductor for typical ferroelectric heterostructures, by assuming the ferroelectric as an insulator.

To explain the experimentally observed instabilities, depolarization instabilities are classified into four categories: the thermodynamic, the coercive-field limited, the resistivity-limited, the extraneous or preparation-limited, i.e., the trap-limited. Among them, the thermodynamic depolarization instability is the conventional depolarization instability, and the most experimental results by far can be explained without this instability.

First, P_s in a ferroelectric formed directly on a semiconductor (F/S) is stable even for a unidomain, i.e., a domain having a lateral dimension much larger than the thickness of the inversion layer. This results holds for typical ferroelectric oxides, e.g., $BaTiO_3$, $KNbO_3$, $PbTiO_3$, and $Bi_4Ti_3O_{12}$, when they are modestly thick, e.g., 200 nm. For this thickness range, the effects of the carrier doping, and the semiconductor band gap have only a secondary effect on the stability, especially for a ferroelectric with a low thermodynamic lin-

ear susceptibility, e.g., $KNbO_3$ and $PbTiO_3$. P_s can also be stable for a short ferroelectric thickness (l_f), e.g., 10 nm even in $BaTiO_3$ which is sensitive to the depolarization instability, although its stability is significantly affected by the above parameters. Combining these results with the recent experiments, we conclude that the most instabilities experimentally observed in F/Ss are nonthermodynamic and extraneous, i.e., limited by traps or disorders at the F/S interface. By overcoming these problems, a FET using F/S structure can be realized practically with no thickness limitation posed by the depolarization instability, e.g., $l_f < 10$ nm and the lateral dimension of single domain ~ 10 nm. Therefore, it should have a great potential for the miniaturization.

An insulating layer between a unidomain insulating ferroelectric and a semiconductor ($F/I/S$) induces a severe depolarization instability much larger than conventionally expected, if there are no surface states at the F/I interface. The stability of P_s in a $F/I/S$ without the surface states is determined mainly by the thermodynamic liner susceptibility but not by the magnitude of bulk P_s. Furthermore, the effective value of the former is predicted to be adjusted by changing the orientation of $P_s(\varphi)$ to suppress the depolarization instability. A thin film of a unidomain ferroelectric phase cannot virtually exist in an ideal $F/I/S$ without defects for $\varphi < 60°$. Moreover, the multidomain formation can explain the ferroelectric stability only at $l_f > 150$ nm for $l_d \geqslant 5$ nm and the net $D=0$. On the other hand, the disorders and the defects at the F/I interface render P_s monostable. However, the experimental values of D and single domain-like properties in $F/I/S$ can be explained by assuming the formation of a conductive layer at F/I or an appropriate density of charged defects.

The instability in $F/I/S$ is drastically modified by introduction of metallic layer between the ferroelectric and the insulator ($F/M/I/S$). Namely, the thermodynamic depolarization instability is removed by the reduction of the net D via multidomain formation. This D is of order 1 μC cm^{-2} and determined by a domain wall pinning, i.e., coercive field. Furthermore, the finite conductivity of the ferroelectric extinguishes this D, if used in integrated circuits or in a short-circuited condition, which explains the experimentally observed short retention of the device using this structure. The coercive-field and resistivity-limited depolarization instabilities dominating in $F/M/I/S$ are nonthermodynamic and do not occur in F/S. Additionally, the application of the present results to an insulating ferroelectric powder suggests that an insulating layer on its surface changes its size effect drastically. This implies that the finite size effect of ferroelectric powder is very sensitive to sample preparation.

Numerical results are analytically explained by Eqs. (11c), (11d), (12b), and (13). The fact that the experimental results for $F/I/S$ was explained only by assuming a narrow range of the interfacial defect density may indicate that the difficulty of the assumption of an *insulating ferroelectric under an enormous depolarization field*.

ACKNOWLEDGMENT

This work was performed under the support through Grant-in-aid for Scientific Research from the Ministry of Education, Science, and Sports. The author acknowledges useful discussion with Professor S. Uchida, Professor T. Yamada, and Professor Y. Ishibashi.

APPENDIX I

We consider a F/S structure similar to Fig. 12, where $\mathbf{P}(y)=P\mathbf{x}$ for $(a+b)n<y<(a+b)n+a$ and $\mathbf{P}(y)=-P\mathbf{x}$ for $(a+b)n+a<y<(a+b)(n+1)$ ($\mathbf{x}$: unit vector in the x direction, n:integer). Here we assume that the 180° domain wall width is negligibly shorter than domain widths a and b. The potential at the metal electrode is assumed to be zero, without loosing generality, and we introduce the potential in the ferroelectric ϕ_f. Because we assume the ferroelectric as an insulator and P as homogeneous ($\nabla P=0$), ϕ_f satisfies the Laplace equation,

$$\Delta\phi_f(x,y)=0,$$

with boundary conditions,

$$\phi(l_f,y)=0, \quad \phi(0,y)=\Psi_s[D(y)]=\Psi_s\{D[P(y)]\}.$$

The second boundary condition is the continuity of the potential where D is related with Eq. (6a). Because of $l_d=0$, we only need to estimate the depolarization term and the semiconductor changing term (F_s) in Eq. (1) as electrostatic energies. For an undoped semiconductor, F_s is approximately the same for the multidomain and the unidomain, if the domain width is sufficiently larger than the domain wall width. Therefore, we can compare the total electrostatic energies for the unidomain and the multidomain by estimating only the conventional depolarization term $\int_0^P dP E_f$.

For multidomain, this is changed to

$$1/[(a+b)l_f]\int_0^{a+b}dy\int_0^{l_f}dx\int_0^{\mathbf{P}(x,y)}d\mathbf{P}\cdot\mathbf{E}_f(x,y,\mathbf{P}).$$

This is rewritten as,

$$1/[(a+b)l_f]\int_0^{a+b}dy\int_0^{l_f}dx\int_0^{P(y)}dP[-\partial\phi_f/\partial x(x,y,P)]$$

$$=1/[(a+b)l_f]\int_0^{a+b}dy\int_0^{P(y)}dP\,\phi_f(0,y,P)$$

$$=1/[(a+b)l_f]\left[a\int_0^P dP\,\phi_f(0,a^-,P)+b\int_0^{-P}dP\,\phi_f(0,a^+,P)\right].$$

The two integrals by P in the last equation give the same values and, we obtain,

$$1/l_f\int_0^P dp\,\phi_f(0,a^-,p)=1/l_f\int_0^P dp\,\Psi_s[D(P)].$$

The final result shows that the depolarization energy is independent of a and b, i.e., the domain structure. The equality $\|\mathbf{P}(y)\|=P$ for $0<y<a$ and $a<y<a+b$ is rigorously correct for an intrinsic semiconductor. When the semiconductor is doped, there is a difference between $\|\mathbf{P}(y)\|$ for

$0<y<a$ and $\|\mathbf{P}(y)\|$ for $b<y<a+b$. However, this difference is very small as seen in the numerical results of a unidomain calculation in the Sec. III.

If we include the effect of the finite thickness of domain width and the space charge layer, a multidomain state should be slightly more stable than a unidomain state. However, a unidomain state can be virtually stable as long as the depolarization field is smaller than the coercive field.

Similarly, the multidomain contribution to the depolarization energy should also be negligible in $F/I/S$ structures, when the thickness of the insulating layer is much thinner than domain widths a and b. For $1_d \gg a,b$, the domain configuration with $a=b$ seems to be only stable and discussed later. The multidomain effect should also dominate in the $F/M/I/S$ structures, and its ferroelectric stability can be simply analyzed.

APPENDIX II: DERIVATION OF EQ. (14)

First, we derive the expression for wall energy. F_f for ferroelectric film is given by

$$F_f = F_0 + \eta(\nabla P)^2 = F_0 + F_d,$$

where the lateral dimension of ferroelectric is much larger than the domain size a.

The domain wall energy F_w per domain wall area is,

$$F_w = \int_{-\infty}^{\infty} \{F_f[P(x) - F_f(P)]dx$$

$$= (-2\alpha_1 P^2 - 8/3\alpha_{11}P^4 - 46/15\alpha_{111}P^6)\xi + 4\eta P^2/3\xi\},$$

where $P(x)$ is assumed as $P\ \tanh(x/\xi)$.[46,10] The half domain width ξ which minimize domain wall energy is given by $\partial\gamma/\partial\xi = 0$. This is satisfied for

$$\xi = \sqrt{[4\eta/3(-2\alpha_1 P^2 - 8/3\alpha_{11}P^4 - 46/15\alpha_{111}P^6)]},$$

yielding the minimum $F_w = \gamma = 8\eta P^2/3\xi$. The material constant η is estimated by equating ξ with the experimentally determined half domain-width in bulk ferroelectric. The expressions of γ and ξ give the wall energy for arbitrary l_f.

Now, we derive the solution of Ψ for multidomain ferroelectric/insulator/metal in Fig. 12. The potential Ψ at the top metal electrode is set to be zero. Because we assume the ferroelectric as insulating and P as homogeneous ($\nabla P = 0$), Ψ satisfies the Laplace equation in the ferroelectric and the insulator,

$$\Delta\Psi(x,y) = 0,$$

with the boundary conditions,

$$\Psi(0,y) = \partial\Psi(0,y)/\partial y = 0,$$

$$\Psi(l_f + l_d, y) = \partial\Psi(l_f + l_d, y)/\partial y = 0,$$

$$\Psi(l_f^+, y) = \Psi(l_f^-, y),$$

$$-\epsilon_d\epsilon_0\partial\Psi(l_f^+, y)/\partial x = -\epsilon_0\partial\Psi(l_f^-, y)/\partial x + P.$$

Fourier series of the solution of Ψ for $0 \leqslant x \leqslant l_f$ is,

$$\Psi(x,y) = c_2 x + \sum \sinh n\kappa x(c_n \cos n\kappa y + s_n \sin n\kappa y),$$

where Σ means sum over n $(1,2,...,\infty)$ and κ is defined as,

$$\kappa = \pi/a.$$

Using this equation, the derivative at $x = l_f$ is given,

$$-\partial\Psi(l_f^-, y)/\partial x = -c_2 - \sum n\kappa \cosh n\kappa l_f(c_n \cos n\kappa y + s_n \sin n\kappa y).$$

P is also expressed in a Fourier series,

$$P = 2P\sum [\sin n\kappa a \cos n\kappa y + (1 - \cos n\kappa a)\sin n\kappa y]/n\kappa a.$$

Fourier series of the solution of Ψ for $l_f \leqslant x \leqslant l_f + l_d$ is,

$$\Psi(x,y) = c_1(x - l_f - l_d) + \sum \sinh n\kappa(x - l_f - l_d) \times (C_n \cos n\kappa y + S_n \sin n\kappa y).$$

Using this expression, Ψ and the derivative at $x = l_f$ are given,

$$-\partial\Psi(l_f^+, y)/\partial x = -c_1 + \sum n\kappa \cosh n\kappa l_d(C_n \cos n\kappa y + S_n \sin n\kappa y),$$

$$\Psi(l_f^+, y) = -c_1 l_d - \sum \sinh n\kappa l_d(C_n \cos n\kappa y + S_n \sin n\kappa y).$$

Combing these results with the boundary condition, we have,

$$c_2 = c_1 = 0, \quad c_n = r_n a \sin n\kappa a \sinh n\kappa l_d/n^2\epsilon_0,$$

$$s_n = r_n a(1 - \cos n\kappa a)\sinh n\kappa l_d/n^2\epsilon_0,$$

$$C_n = -r_n a \sin n\kappa a \sinh n\kappa l_f/n^2\epsilon_0,$$

$$S_n = -r_n a(1 - \cos n\kappa a)\sinh n\kappa l_f/n^2\epsilon_0,$$

where r_n is defined as

$$r_n = 2P/[\pi^2(\epsilon_d \cosh n\kappa l_d \sinh n\kappa l_f + \cosh n\kappa l_f \sinh n\kappa l_d)].$$

At large n, we have

$$n^{-3} r_n \sinh n\kappa l_f \sinh n\kappa l_d \sim 2Pn^{-3}/\pi^2(\epsilon_d + 1),$$

$$n^{-3} r_n^2 \epsilon_d \sinh^2 n\kappa l_f \sinh 2\, n\kappa l_d \sim 4P^2 n^{-3}\epsilon_d/\pi^4(\epsilon_d + 1)^2.$$

This assures a fast convergence of the sums Eqs. (14a) and (14b).

[1] H. L. Stadler, J. Appl. Phys. **33**, 3487 (1962).
[2] A. J. Bell, Ferroelectr. Lett. Sect. **15**, 133 (1993).
[3] T. Yamamoto, Integr. Ferroelectr. **12**, 161 (1996).
[4] T. Yamamoto, K. Urabe, and H. Banno, Jpn. J. Appl. Phys., Part 1 **32**, 4247 (1993).
[5] W. R. Kretschmer and K. Binder, Phys. Rev. B **20**, 1065 (1979).
[6] K. Binder, Ferroelectrics **35**, 99 (1981).
[7] D. R. Tilley and B. Zeks, Solid State Commun. **49**, 823 (1984).
[8] X. L. Zhong, B. D. Qu, P. L. Zhang, and Y. G. Wang, Phys. Rev. B **50**, 12 375 (1994).
[9] G. Arlt, D. Hennings, and G. de With, J. Appl. Phys. **58**, 1619 (1985).

[10] W. Y. Shih, W. H. Shih, and I. A. Aksay, Phys. Rev. B **50**, 15 575 (1994).
[11] M. H. Lee, A. Halliyal, and R. E. Newnham, Ferroelectrics **87**, 71 (1988).
[12] B. M. Vul, G. M. Guro, and I. I. Ivanchik, Sov. Phys. Semicond. **4**, 128 (1970).
[13] G. M. Guro, I. I. Ivanchik, and N. F. Kovtonyuk, Sov. Phys. Solid State **11**, 1574 (1970).
[14] I. P. Batra, P. Wurfel, and B. D. Silverman, Phys. Rev. B **8**, 3257 (1973).
[15] P. Wurfel and I. P. Batra, Phys. Rev. B **8**, 5126 (1973).
[16] I. P. Batra, P. Wurfel, and B. D. Silverman, Phys. Rev. Lett. **30**, 384 (1973).
[17] J. L. Moll and Y. Tarui, IEEE Trans. Electron Devices **10**, 338 (1963).
[18] P. M. Heyman and G. H. Heilmeier, Proc. IEEE **54**, 842 (1965).
[19] R. Zuleeg and H. H. Weider, Solid-State Electron. **9**, 657 (1966).
[20] S. S. Perlman and K. H. Ludewig, IEEE Trans. Electron Devices **14**, 814 (1967); J. H. McCusker and S. S. Perlman, *ibid.* **15**, 182 (1968).
[21] G. G. Teather and L. Young, Solid-State Electron. **11**, 527 (1968).
[22] J. C. Crawford and F. L. English, IEEE Trans. Electron Devices **16**, 525 (1969).
[23] S. Y. Wu, IEEE Trans. Electron Devices **21**, 499 (1974).
[24] K. Sugibuchi, Y. Kurogi, and N. Endo, J. Appl. Phys. **46**, 2877 (1975).
[25] T. A. Rost, H. Lin, and T. A. Rabson, Appl. Phys. Lett. **59**, 3654 (1991).
[26] D. R. Lampe, D. A. Adams, M. Austin, M. Polinsky, J. Dzimianski, S. Sinharoy, H. Buhay, P. Brabant, and Y. M. Liu, Ferroelectronics **133**, 61 (1992).
[27] T. Hirai, K. Teramoto, T. Nishi, T. Goto, and Y. Tarui, Jpn. J. Appl. Phys., Part 1 **33**, 5219 (1994); T. Hirai, K. Teramoto, K. Nagashima, H. Koike, and Y. Tarui, *ibid.* **34**, 4163 (1995).
[28] T. Nakamura, Y. Nakao, A. Kamisawa, and H. Takatsu, Dig. Tech. Pap. IEEE International Solid-State Circuits Conference, 1995 (unpublished); Y. Nakao, T. Nakamura, A. Kamisawa, and H. Takasu, Integr. Ferroelectr. **6**, 23 (1995).
[29] E. Tokumitsu, K. Itani, B. Moon, and H. Ishihara, J. Appl. Phys. **34**, 5202 (1995).
[30] C. H. Seager, D. McIntyre, B. A. Tuttle, and J. Evans, Integr. Ferroelectr. **6**, 47 (1995).
[31] Y. Watanabe, Appl. Phys. Lett. **66**, 1770 (1995).
[32] Y. Watanabe, M. Tanamura, and Y. Matsumoto, Jpn. J. Appl. Phys., Part 1 **35**, 1564 (1996).
[33] For example, K. Iijima, T. Terashima, K. Yamamoto, K. Hirata, and Y. Bando, J. Appl. Phys. **56**, 527 (1990).
[34] K. Abe and K. Komatsu, Jpn. J. Appl. Phys., Part 1 **32**, 4186 (1993).
[35] T. Hase, T. Sakuma, Y. Miyasaka, K. Hirata, and N. Hosokawa, Jpn. J. Appl. Phys., Part 1 **32**, 4061 (1993).
[36] M. Kiyotoshi and K. Eguchi, Appl. Phys. Lett. **67**, 2468 (1995).
[37] Y. Watanabe, Y. Matsumoto, H. Kunitomo, M. Tanamura, and E. Nishimoto, Jpn. J. Appl. Phys., Part 1 **33**, 5182 (1994).
[38] S. L. Miller and P. J. McWhorter, J. Appl. Phys. **72**, 5999 (1992).
[39] Y. Watanabe, Phys. Rev. B **57**, 789 (1998).
[40] A. F. Devonshire, Philos. Mag. **40**, 1065 (1951).
[41] M. J. Haun, E. Furman, S. J. Jang, H. A. Kinstry, and L. E. Cross, J. Appl. Phys. **62**, 3331 (1987); T. Yamamoto and H. Matsuoka, Jpn. J. Appl. Phys., Part 1 **33**, 5317 (1994).
[42] W. Känzig, *Solid State Physics 4*, edited by E. Seitz and D. Turnbull (Academic, New York, 1957).
[43] L. E. Cross and R. C. Pohanka, Mater. Res. Bull. **6**, 939 (1971).
[44] B. E. Deal, E. W. Snow, and C. A. Mead, J. Phys. Chem. Solids **27**, 1873 (1966); W. M. Werner, Solid-State Electron. **17**, 769 (1974).
[45] S. M. Sze, *Physics of Semiconductor Devices* (Wiley, New York, 1981).
[46] M. E. Lines and A. M. Glass, *Principles and Applications of Ferroelectric and Related Materials* (Oxford University Press, Oxford, 1977).
[47] E. Jona and G. Shirane, *Ferroelectric Crystals* (Pergamon, New York, 1962).
[48] C. Kittel, Rev. Mod. Phys. **21**, 541 (1949); S. Chikazumi, in *Physics of Ferromagnetism* (in Japanese, Syokabo, Tokyo, 1984), Vol. 2, p. 193.
[49] P. Güthner and K. Dransfeld, Appl. Phys. Lett. **61**, 1139 (1992); K. Frank, J. Besold, W. Haessler, and C. Seegebarth, Surf. Sci. Lett. **302**, 283 (1994).
[50] W. Känzig, Phys. Rev. **98**, 549 (1955).
[51] G. Heiland, Z. Phys. **148**, 28 (1957); P. E. Bloomfield, I. Lefkowitz, and A. D. Aronoff, Phys. Rev. B **4**, 974 (1971).
[52] Y. Watanabe and D. Sawamura, Jpn. J. Appl. Phys., Part 1 **36**, 6162 (1997).
[53] Y. Watanabe, Y. Matsumoto, and M. Tanamura, Jpn. J. Appl. Phys., Part 1 **34**, 5254 (1995).